Neuroscience Letters 756 (2021) 135956

Contents lists available at ScienceDirect

Neuroscience Letters

journal homepage: www.elsevier.com/locate/neulet

Comparative study of neuron-specific promoters in mouse brain transduced by intravenously administered AAV-PHP.eB

Putri T. Radhiyanti [a,c], Ayumu Konno [a,b], Yasunori Matsuzaki [a,b], Hirokazu Hirai [a,b,*]

[a] Department of Neurophysiology and Neural Repair, Gunma University Graduate School of Medicine, 3-39-22, Gunma, 371-8511, Japan
[b] Viral Vector Core, Gunma University Initiative for Advanced Research (GIAR), Gunma, 371-8511, Japan
[c] Department of Biomedical Science, Faculty of Medicine, Universitas Padjadjaran, Bandung, Indonesia

ARTICLE INFO

Keywords:
Adeno-associated virus
AAV-PHP.B
Neuron-specific promoter
CaMKII promoter
NSE promoter
Synapsin I promoter

ABSTRACT

Adeno-associated virus (AAV)- PHP.B and AAV-PHP.eB (PHP.eB), a capsid variant of AAV serotype 9, efficiently penetrates the mouse blood-brain barrier and predominantly infects neurons. Thus, the PHP.B / PHP.eB capsid and a neuron-specific promoter is a reasonable combination for effective neuronal transduction. However, the transduction characteristics of intravenously administered PHP.B / PHP.eB carrying different neuron-specific promoters have not been studied systematically. In this study, using an intravenous infusion of PHP.eB in mice, we performed a comparative study of the ubiquitous CBh and three neuron-specific promoters, the Ca^{2+}/calmodulin-dependent kinase subunit α (CaMKII) promoter, neuron-specific enolase (NSE) promoter, and synapsin I with a minimal CMV sequence (SynI-minCMV) promoter. Expression levels of a transgene by three neuron-specific promoters were comparable to or higher than those of the CBh promoter. Among the promoters examined, the NSE promoter showed the highest transgene expression. All neuron-specific promoters were activated specifically in the neurons. PHP.eB carrying the CaMKII promoter, which is generally believed to exert its function exclusively in the excitatory neurons, transduced both the excitatory and inhibitory neurons without bias, whereas PHP.eB with the NSE and SynI-minCMV promoters transduced neurons with significant bias toward inhibitory neurons. These results are useful in neuron-targeted broad transgene expression through systemic infusion of blood-brain-barrier-penetrating AAV vectors carrying the neuron-specific promoter.

1. Introduction

The adeno-associated virus (AAV) vector is a small, non-enveloped, non-pathogenic, single-stranded DNA parvovirus that infects various cell types, including numerous types of neurons and glia. Thirteen naturally occurring AAV serotypes of human and simian origin have been reported [1], which are recognized by distinct cell-surface receptors and have different cellular affinities [2]. For example, astrocytes are the dominant cell type transduced by AAV serotype 8, whereas AAV serotype 9 (AAV9) predominantly transduces neurons, despite using the same cytomegalovirus (CMV) promoter [3]. Another crucial determinant of cell types transduced by AAV vectors is the incorporated promoter or enhancer. The astrocyte-specific GFAP promoter drives transgene expression exclusively in astrocytes, even if neuron-tropic AAV9 is used for transgene delivery [4,5]. Thus, profiles of cell types transduced by different AAV vectors depend on the capsid type and promoter/enhancer incorporated into the viral vectors.

Deverman et al. reported AAV-PHP.B (hereafter, PHP.B), a capsid variant of AAV9 with insertion of 7 amino acids, which displayed an extremely high capacity for penetration through the mouse blood-brain barrier (BBB) [6]. Intravenous infusion of PHP.B resulted in efficient transduction of the whole brain. In addition, the same group engineered AAV-PHP.eB (hereafter, PHP.eB), which differed by only 2 amino acids from PHP.B at the position adjacent to the heptamer insertion site [7].

Abbreviations: AAV, adeno-associated virus; AAV9, adeno-associated virus serotype 9; BBB, blood-brain barrier; CaMKII, Ca^{2+}/calmodulin-dependent kinase subunit α; CBh, chicken β-actin hybrid; CMV, cytomegalovirus; E/I, excitatory neuron to inhibitory neuron; GABA, gamma-aminobutyric acid; GFAP, glial fibrillary acidic protein; GFP, enhanced green fluorescent protein; LY6a, lymphocyte antigen 6 complex, locus A; NSE, neuron-specific enolase; SV40pA, simian virus 40 polyadenylation signal; SynI-minCMV, Synapsin I minimal CMV; VGAT, vesicular GABA transporter; WPRE, woodchuck hepatitis virus posttranscriptional regulatory element.

* Corresponding author at: Department of Neurophysiology and Neural Repair, Gunma University Graduate School of Medicine, 3-39-22, Gunma, 371-8511, Japan.
E-mail address: hirai@gunma-u.ac.jp (H. Hirai).

https://doi.org/10.1016/j.neulet.2021.135956
Received 17 January 2021; Received in revised form 7 May 2021; Accepted 9 May 2021
Available online 11 May 2021

Intravenous injection of PHP.eB resulted in significantly increased transduction and higher transduction efficiency for neurons in the cerebral cortex than PHP.B [7]. These results suggest that the AAV-PHP.eB, and a neuron-specific promoter is an ideal combination for efficient transduction of cortical neurons. To restrict transgene expression to neurons, numerous neuron-specific promoters, including the Ca^{2+}/calmodulin-dependent kinase type II subunit α (CaMKII) promoter, neuron-specific enolase (NSE) promoter, and synapsin I promoter, have been used for AAV vectors [8–10]. However, the transduction profiles of intravenously infused AAV-PHP.eB carrying these promoters have not been studied; hence, it remains unclear which promoter is the most optimal and which should be used for designed experiments. In the present study, to obtain the characteristics of PHP.eB with different neuron-specific promoters, we performed a comparative study of three neuron-specific promoters by intravenously infusing AAV-PHP.eB harboring either one of the promoters in terms of promoter strength and transduction ratios of neurons versus non-neuronal cells and those of excitatory versus inhibitory neurons, respectively.

2. Material and methods

2.1. Animals

All animal procedures were performed in accordance with the institutional and national guidelines and were approved by the Gunma University Animal Care and Experimental Committee (18–019 and 20–047). Adult male or female wild-type and vesicular GABA transporter (VGAT)-tdTomato mice [11], which were kindly provided by Dr. Ryosuke Kaneko at Osaka University, were used in this study.

2.2. Viral vector

The expression plasmids, pAAV/CBh-GFP-WPRE-SV40pA, pAAV/mCaMKII-GFP-WPRE-SV40pA, and pAAV/SynI-mCMV-GFP-WPRE-SV40pA, were obtained by the substitution of the NSE promoter in pAAV/NSE(1.2k)-GFP-WPRE-SV40pA [12] for each promoter at restriction enzyme sites for XhoI and AgeI. Rep/Cap packaging plasmid pAAV-PHP.B and pAAV-PHP.eB, were constructed from the pAAV2/9 plasmid, which was provided by Dr. James M. Wilson at the University of Pennsylvania. Recombinant single-strand AAV-PHP.B/PHP.eB vectors were produced using the ultracentrifugation method described in a previous paper [13].

2.2.1. Viral injection

Mice were deeply anesthetized with a combination of ketamine and xylazine before intravenous injection. Intravenous injection of the viral vector was performed into the orbital sinus using a 0.5 mL syringe with a 30-gauge needle (Nipro, Osaka, Japan). Each viral vector (100 μL) (2.0×10^{12} viral genome (vg) / mL) was injected intravenously into a mouse. All mice were euthanized 2 weeks post-injection, perfused transcardially with 1 × PBS (-), and fixed with 4% paraformaldehyde (PFA) in 0.1 M phosphate buffer (PB). The brains were harvested and incubated in 4% PFA solution for 6–8 h at 4 °C.

2.3. GFP fluorescence intensity measurement

GFP fluorescence images of the whole brain were acquired using a fluorescence stereoscopic microscope (VB-7010; Keyence, Osaka, Japan). GFP fluorescence intensity of the whole brain, cerebrum, and cerebellum was measured using ImageJ software. The outline of each area was traced, and the fluorescence intensity in the enclosed areas was measured accordingly. The background intensity was subtracted from fluorescence intensity. The intensity ratio of each group was calculated as the average intensity of the AAV-PHP.eB/CBh group.

2.4. Immunohistochemistry

The brains were cut sagitally into 50-μm-thick sections using a vibrating blade microtome (VT1200S; Leica, Wetzlar, Germany). Floating brain sections were then permeabilized and blocked in blocking solution containing 0.5 % Triton X-100, 2 % bovine serum albumin, 2 % normal donkey serum, 0.05 % NaN_3, and 0.1 M phosphate buffer, overnight at room temperature (24–26 °C) with the following primary antibodies: rat monoclonal anti-GFP (1:1000; 04404–84; Nacalai Tesque, Kyoto, Japan), rabbit polyclonal anti-DsRed (1:1000; #632496; Takara Bio, Mountain View, CA, USA), and mouse monoclonal anti-NeuN (1:1000; MAB377; Merck, Darmstadt, Germany). The primary antibodies were visualized after incubation with Alexa Fluor 488-conjugated donkey anti-rat IgG (1:1000; Thermo Fisher Scientific, Waltham, MA, USA), Alexa Fluor 568-conjugated donkey anti-rabbit IgG (1:1000; Thermo Fisher Scientific), and Alexa Fluor 647-conjugated donkey anti-mouse IgG (1:1000; Thermo Fisher Scientific) in blocking solution for 3 h at room temperature. Cell nuclei were stained with Hoechst 33342 for 25 min to identify the cells in the brain sections of control mice. The slices were then mounted using Prolonged Diamond Antifade Reagent (P36961; Thermo Fisher Scientific).

2.5. Cell quantification

For cell counting, fluorescent images of the motor cortex, striatum, and CA1, CA2, and CA3 regions of the hippocampus were obtained using a laser-scanning confocal microscope (LSM 800, Carl Zeiss, Oberkochen, Germany) with a 20× objective. Cell numbers were counted manually using Fiji ImageJ software in each tested promoter and control group (three slices per mouse, n = 5–6 mice). NeuN-positive cells were counted as neurons. NeuN- and DsRed-positive cells were counted as inhibitory neurons. NeuN-positive, but DsRed-negative cells were counted as excitatory neurons.

2.6. Statistical analysis

GraphPad PRISM version 9 (GraphPad Software, San Diego, CA, USA) was used for the statistical analysis and production of graphic images. The *t*-test was used for conducting a comparative analysis between non-injected control and PHP.B/CBh and between PHP.B/CBh and PHP.eB/CBh. One-way analysis of variance together with Dunnet's or Tukey's post-hoc test was used for performing a comparative analysis between the non-injected control group and all PHP.eB groups. $P < 0.05$ was regarded as statistically significant.

3. Results

3.1. Greater GFP expression by intravenous injection of PHP.eB over of PHP.B

PHP.B or PHP.eB expressing GFP under the control of the chicken β-actin hybrid (CBh) promoter was intravenously injected into 5–7-week-old VGAT-tdTomato mice at the same viral titer (2.0×10^{12} vg/mL) (Fig. 1A). Two weeks after the injection, the mice were sacrificed, and native GFP fluorescent images of the whole brain were captured using fluorescent stereoscopic microscopy (Fig. 1B). We measured GFP fluorescence intensity in the whole brain, cerebrum, and cerebellum. Statistical analysis by unpaired *t*-test showed significantly higher GFP intensity in PHP.eB-treated brains than in those treated with PHP.B ($p = 0.0238$, 0.0411, and 0.0008 in the whole brain, cerebrum, and cerebellum, respectively) (Fig. 1C). These results indicate that PHP.eB penetrates the BBB more effectively and/or enters brain cells more efficiently than PHP.B, thus confirming the findings of a previous study [7,14].

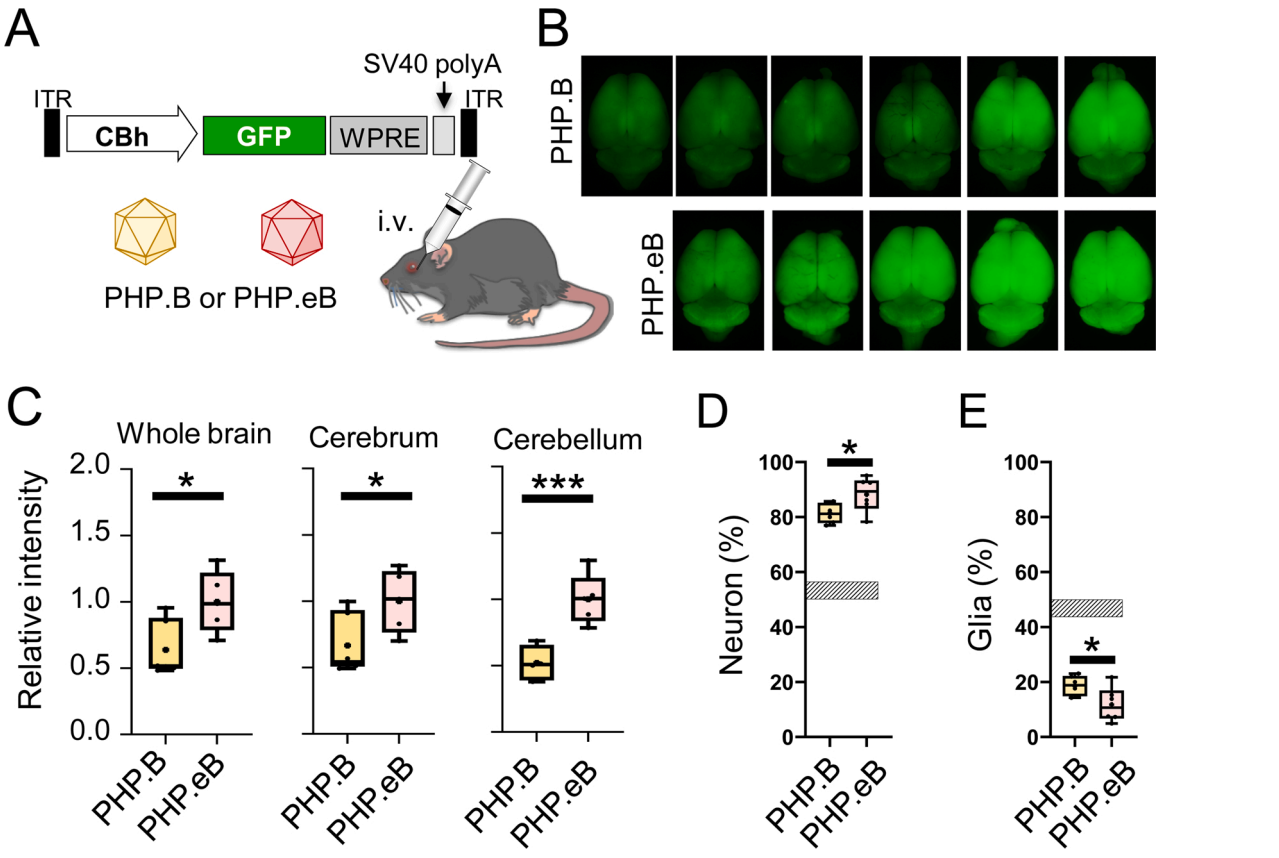

Fig. 1. Comparison of AAV-PHP.B (PHP.B) and AAV-PHP.eB (PHP.eB) in the brain transduction.
(A) Mice received intravenous injection of PHP.B or PHP.eB expressing GFP under the control of the non-specific CBh promoter. (B) GFP fluorescent image of the whole brain 2 weeks after the PHP.B (upper images) or PHP.eB (lower images) injection. (C) Quantitative analysis of the GFP fluorescent intensity in the whole brain (left), cerebrum (middle) and cerebellum (right) that were treated with PHP.B or PHP.eB. (D, E) Percentage of neurons (D) and glial cells (E) in transduced cells. Sagittal sections of the whole brains (B) were immunolabeled for NeuN. NeuN-positive and -negative parenchymal cells were counted as neurons and glial cells, respectively. Shaded area in the graph represents natural ratio of neurons or glia to total parenchymal cells. $*p < 0.05$ by unpaired *t*-test.

3.2. Both PHP.B and PHP.eB transduce neurons more effectively than non-neuronal cells

Sagittal brain sections from mice that received intravenous infusion of PHP.B or PHP.eB were double immunolabeled with antibodies against NeuN, a neuronal marker, and Hoechst 33342 for nuclear labeling (Supplementary Fig. 1). We first examined the proportion of neurons and non-neuronal cells in the total parenchymal cells of the motor cortex from non-injected control mice, and found 53.0 ± 2.9 % of cells as NeuN-positive neurons and 47.0 ± 2.9 % of cells as NeuN-negative non-neuronal cells. Next, we examined the ratio of transduced neurons to whole transduced (GFP-expressing) cells in the motor cortex of virally treated mice. Cells double labeled for GFP and NeuN (namely, neurons) accounted for 81.4 ± 1.5 % and 88.2 ± 2.6 % of whole GFP-expressing cells in the motor cortex from mice treated with PHP.B or PHP.eB, respectively (Fig. 1D and Supplementary Table 1 for detailed information on numbers of mice and cells counted). The ratios of transduced neurons to whole transduced cells (81.4 % and 88.2 %) were significantly higher than the natural ratio of neurons to whole parenchymal cells (neurons + non-neuronal cells) (53.0 %; shaded area in Fig. 1D). These results suggested that both PHP.B-and PHP.eB-transduced neurons were more effective than non-neuronal cells. Consistent with previous studies [7,14], the ratio of transduced neurons to whole transduced cells was significantly higher in PHP.eB-treated mice than in PHP.B-treated mice ($p = 0.0439$ by paired *t*-test), suggesting a slight, but significantly greater advantage of using PHP.eB over PHP.B in the transduction of neurons. Thus, we used PHP.eB in subsequent experiments aimed at neuronal transduction.

3.3. The NSE promoter shows highest promoter strength in the cerebral cortex

An intravenous administration of neuron-tropic PHP.eB vectors with a neuron-specific promoter such as the CaMKII promoter [15], NSE promoter [12], and SynI-minCMV promoter [16] likely causes highly efficient neuronal transduction in the whole brain. However, few studies have systematically examined the characteristics of these promoters when delivered into the brain using BBB-penetrating AAV vectors. Thus, by intravenously injecting PHP.eB vectors into VGAT-tdTomato mice expressing tdTomato specifically in inhibitory GABAergic neurons [11], we compared the transduction features of the neuron-specific promoters (CaMKII, NSE, and SynI-minCMV promoters) (Fig. 2A) in terms of promoter strength and specificity to excitatory and inhibitory neurons. VGAT-tdTomato mice received either one of the PHP.eB vectors (100 μL, 2.0×10^{12} vg/mL). PHP.eB carrying the CBh promoter was used as a control. The brains of these mice were examined 2 weeks after viral injection. We found the brightest GFP signal from the brains treated with PHP.eB carrying the NSE promoter (Fig. 2B), and this finding was confirmed by quantitative analysis; the NSE promoter contributed to the highest levels of GFP expression in the whole brain and the cerebrum, compared with those in the other three promoters (left and middle graphs, respectively, in Fig. 2C). In the cerebellum, the CBh promoter and NSE promoter caused comparable levels of GFP expression, while the CaMKII promoter and SynI-minCMV promoter resulted in lower levels of GFP expression (Fig. 2C, right).

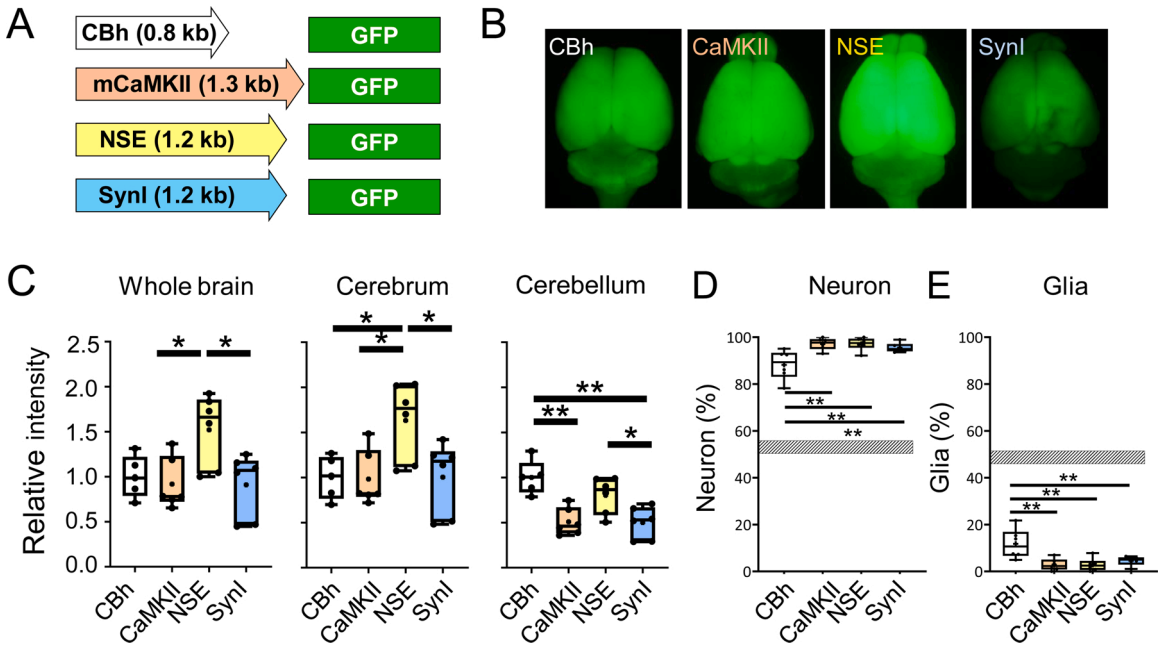

Fig. 2. Comparison of transduction profiles of the brains intravenously treated with PHP.eB expressing GFP under the control of 3 different neuron-specific promoters.

(A) Scheme depicting relative size of 3 neuron-specific promotrs, mouse Ca^{2+}/calmodulin-dependent protein kinase II promoter (mCaMKII), neuron-specific enolase promoter (NSE), synapsin I promoter with a minimal CMV sequence (Syn I), and non-selective CBh promoter (CBh). Each promoter size is shown in parenthesis. (B) GFP fluorescent image of the whole brain 2 weeks after intravenous infusion of PHP.eB carrying either one of promoters depicted in (A). (C) Quantitative analysis of the GFP fluorescent intensity in the whole brain (left), cerebrum (middle) and cerebellum (right) that were treated with PHP.eB carrying a promoter as described. (D, E) Percentage of neurons (D) and glial cells (E) in transduced cells. Sagittal sections of the whole brains (B) were immunolabeled for NeuN. Proportion of NeuN-positive neurons and that of NeuN-negative glial cells to total parenchymal cells were determined. Shaded area in the graph represents natural ratio of neurons or glia to total parenchymal cells. *$p < 0.05$, **$p < 0.01$ and ***$p < 0.001$ by one-way ANOVA with Dunnett's or Tukey's post hoc test.

3.4. Neuron-specific transduction by PHP.eB carrying a neuron-specific promoter in the cerebral cortex

We produced sagittal brain sections to examine whether neuron-specific promoters drove transgene expression specifically in neurons in the cerebral cortex, when intravenously administered with PHP.eB. The sections were double-immunolabeled for NeuN (Supplementary Fig. 2) and tdTomato with anti-DsRed antibody, which cross-reacts with tdTomato, to enhance the labeling of the inhibitory neurons (Supplementary Fig. 3). As expected, over 95 % of cells transduced by PHP.eB carrying neuron-specific promoters were identified as neurons, which was significantly higher than the value (88.2 %) by the ubiquitous CBh promoter (Fig. 2D, E and Supplementary Table 2).

Next, we examined the proportion of excitatory neurons (NeuN-positive and DsRed-negative) and inhibitory neurons (DsRed-positive) in all transduced (GFP-expressing) cells. In the motor cortex of non-injected control mice, excitatory and inhibitory neurons accounted for ~46 % and ~8% of the total parenchymal cells, respectively (Table 1). The ratio of excitatory neurons to cells transduced by PHP.eB carrying the CBh promoter was 78.8 ± 2.6 %, which was significantly higher than the proportion of excitatory neurons in the total parenchymal cells of the motor cortex (45.5 ± 2.5 %). Conversely, the proportion of inhibitory neurons to total transduced cells by PHP.eB carrying the CBh promoter (9.4 ± 1.1 %) was almost similar to the natural proportion of inhibitory neurons in the parenchymal cells (7.5 ± 0.4 %, Table 1), suggesting that PHP.eB carrying the CBh promoter preferentially transduced excitatory rather than inhibitory neurons. PHP.eB carrying the CaMKII promoter transduced excitatory and inhibitory neurons in a similar proportion as PHP.eB with the CBh promoter, whereas PHP.eB carrying the NSE promoter and carrying the SynI-minCMV promoter caused a significantly higher transduction ratio of inhibitory neurons to total transduced cells (over 20 %), compared to the natural proportion of inhibitory neurons in the total parenchymal cells of the motor cortex (7.5 ± 0.4 %, Table 1).

We measured the ratio of excitatory neurons to inhibitory neurons (E/I ratio) in the motor cortex of non-injected control mice, which was 6.1 ± 0.2 (Table 2). The E/I ratios of transduced neurons were higher in the cerebral cortex treated with PHP.eB carrying the CBh promoter (9.2 ± 1.4) or CaMKII promoter (8.0 ± 1.0). Conversely, the E/I ratios of transduced neurons were lower in mice treated with PHP.eB carrying the NSE promoter (4.0 ± 0.7) or SynI-minCMV (3.1 ± 0.3). These results suggest that PHP.eB carrying the CBh and CaMKII promoters tended to

Table 1

VGAT-tdTomato mice received intravenous infusion of PHP.eB expressing GFP under the control of a neuron-specific promoter or ubiquitous CBh promoter. Sagittal brain sections were obtained 2 weeks after the viral injection, and immunostained with anti-NeuN and anti-DsRed antibodies. Proportions of excitatory (NeuN-positive and DsRed-negative) and inhibitory (NeuN-positive and DsRed-positive) neurons and non-neuronal cells (NeuN-negative) to total GFP-expressing cells were determined using 3 slices per mouse, total 6 mice for each promoter. * vs Non-injected control, † vs CBh, ‡ vs CaMKII. One, two, three and four symbols represent p values less than 0.05, 0.01, 0.001 and 0.0001, respectively, by one-way ANOVA with Dunnet's or Tukey's post hoc test.

		Neuron		Non-neuronal (%)
		Excitatory (%)	Inhibitory (%)	
Non-injected control		45.5 ± 2.5	7.5 ± 0.4	47.0 ± 2.9
PHP.eB	CBh	78.8 ± 2.6 ****	9.4 ± 1.1	11.8 ± 2.6 ****
	CaMKII	85.6 ± 2.4 ****	11.6 ± 1.5	2.8 ± 1.0 ****††
	NSE	76.7 ± 3.0 ****	20.5 ± 2.6 ***††‡	2.8 ± 1.1 ****††
	SynI	71.7 ± 2.4 ****‡‡	23.8 ± 2.7 ****††‡‡	4.5 ± 0.8 ****††

*vs Non-injected control, † vs CBh, ‡ vs CaMKII.

Table 2
VGAT-tdTomato mice received intravenous infusion of PHP.eB expressing GFP under the control of a neuron-specific promoter or ubiquitous CBh promoter. Excitatory and inhibitory neurons were determined immunohistochemically as described in the Table 1 legend. * vs Non-injected control,† vs CBh, ‡ vs CaMKII. One, two and three symbols represent p values less than 0.05, 0.01 and 0.001, respectively, by one-way ANOVA with Dunnet's or Tukey's post hoc test.

		Excitatory (%)	Inhibitory (%)	E/I ratio
Non-injected control		85.8 ± 0.4	14.2 ± 0.4	6.1 ± 0.2
PHP.eB	CBh	89.3 ± 1.2	10.7 ± 1.2	9.2 ± 1.4*
	CaMKII	88.1 ± 1.6	11.9 ± 1.6	8.0 ± 1.0
	NSE	78.3 ± 2.5 *††‡	21.7 ± 2.5 *††‡	4.0 ± 0.7 ††‡‡
	SynI	74.5 ± 2.4 ***††‡‡	25.5 ± 2.4 ***††‡‡	3.1 ± 0.3 ††‡‡

*vs Non-injected control, † vs CBh, ‡ vs CaMKII.

cause excitatory neuron-preferential transduction, whereas PHP.eB carrying the NSE and SynI-minCMV promoters transduced neurons with a significant bias for inhibitory neurons.

3.5. Both PHP.B and PHP.eB efficiently transduced the inhibitory neurons in the striatum

Nearly all neurons (99 %) present in the striatum are known to be GABAergic (96 % of the projection neurons and 3% of the interneurons), with the remaining 1% as cholinergic neurons [17]. Thus, it is interesting to investigate the transduction profile of intravenously injected PHP.B/PHP.eB in the striatum. To pursue this, we intravenously injected PHP.B or PHP.eB expressing GFP under the control of the ubiquitous CBh promoter or neuron-specific promoter to wild-type mice. Two weeks after injection, we assessed the ratios of transduced neurons and transduced non-neuronal cells to total transduced cells together with the natural proportion of neurons and non-neuronal cells in the striatum (Supplementary Tables 3 and 4). Neuron bias of PHP.B and stronger neuron bias of PHP.eB over PHP.B in the striatum were similar to the results in the cerebral cortex (Supplementary Table 2). Notably, both PHP.B and PHP.eB efficiently transduced inhibitory neurons in the striatum (Supplementary Table 4).

3.6. Neuron-specific transduction by PHP.B and PHP.eB in the hippocampus

Next, we conducted similar analyses in the hippocampus, using VGAT-tdTomato mice (Supplementary Table 3). Again, we found neuron bias of PHP.B and PHP.eB in the CA1, CA2, and CA3 regions of the hippocampus (Supplementary Table 5). Unlike the cerebral cortex, there was no statistically significant difference between PHP.B and PHP.eB, in terms of neuron bias. Similar to the cerebral cortex, PHP.eB carrying the NSE promoter or SynI-minCMV promoter showed some inhibitory neuron bias, especially in the CA1 region, where PHP.eB carrying the NSE promoter transduced inhibitory neurons with a 10-times higher proportion (~22 %) than the natural presence (2.4 %) (Supplementary Table 5).

4. Discussion

4.1. Higher neuronal transduction by PHP.eB over PHP.B

PHP.B and PHP.eB showed neuron-tropic transduction with significantly higher efficacy in PHP.eB than in PHP.B (Fig. 1D) [7,14]. These results suggest that, while PHP.B and PHP.eB preserve similar tropism as their parent AAV9 for cortical neurons [3,18], the two amino acid differences between PHP.B and PHP.eB at the site adjacent to the heptamer insertion [7] altered the tropism of neurons and/or glia. PHP.eB harboring the CBh promoter transduced both excitatory and inhibitory neurons with significant predominance for excitatory neurons (Table 1), in sharp contrast to inhibitory neuron-preferential transduction by AAV serotype 1 [19]. A similar neuron bias of PHP.B and PHP.eB was also observed in the striatum and hippocampus (Supplementary Tables 4 and 5). Notably, PHP.eB efficiently transduced GABAergic inhibitory neurons in the striatum (Supplementary Table 4). The excitatory neuron bias of the PHP.eB capsid would be an important point when expressing a transgene in cortical and hippocampal neurons via systemic infusion.

4.2. The 1.3 kb CaMKII promoter does not work as an excitatory neuron-specific promoter

By injecting lentiviral vectors into the mouse cerebral cortex, a previous study compared the CaMKII promoter extending three different promoter regions, 0.4, 1.3, and 2.4 kb [15]. The results showed that all three CaMKII promoters restricted expression to cortical pyramidal neurons with a 1.3-kb promoter being the strongest. Although the CaMKII promoter is widely believed to serve as an excitatory neuron-specific promoter, our results showed that intravenously infused PHP.eB harboring the 1.3-kb CaMKII promoter transduced both excitatory and inhibitory neurons with a similar proportion of their natural presence (Table 2). In the striatum, PHP.eB carrying the CaMKII promoter transduced inhibitory neurons with a similar efficacy as that of other promoters (Supplementary Table 5). The excitatory neuron-restricted transduction by lentiviral vectors may be due to the strong tropism of lentiviral vectors for excitatory neurons [19].

4.3. The NSE promoter and SynI-minCMV promoter show a bias toward inhibitory neurons

The NSE promoter and SynI-minCMV promoter transduced significantly more inhibitory neurons (22 %–26 %) than their natural presence (14 %) in the cerebral cortex (Table 2). A similar inhibitory neuron bias of these promoters was observed in the hippocampus (Supplementary Table 5). Why does the NSE promoter show higher promoter activity in inhibitory, rather than excitatory, neurons? NSE, which is expressed at very high levels in neurons, is a glycolytic enzyme at the ninth and penultimate steps of the reaction. Fast-spiking parvalbumin-containing inhibitory neurons are the major inhibitory neuron subtypes, accounting for over 40 % of cortical inhibitory interneurons. During gamma oscillations, parvalbumin-expressing inhibitory neurons fire at a high frequency of over 20 Hz, in contrast to the sparse generation of action potentials at 1–3 Hz in excitatory pyramidal neurons [20,21]. Thus, fast-spiking inhibitory neurons spend much more energy than excitatory pyramidal neurons [21]. To supply cellular energy, glycolytic machinery is enriched in presynaptic compartments [22], where glycolysis produces ATP, which is crucial for the synaptic vesicle cycle, a major consumer of presynaptic ATP [23]. Thus, to meet the high ATP requirement at presynaptic sites, glycolysis is more upregulated in fast-spiking inhibitory neurons than in excitatory pyramidal neurons [21]. Accordingly, it is reasonable to suppose that the NSE promoter is activated more in fast-spiking inhibitory neurons than in excitatory neurons.

Similar to NSE, synapsin I also plays a crucial role in neurotransmitter release from presynaptic terminals. Ablation of synapsin I more profoundly affected inhibitory synaptic transmission than excitatory transmission in cultured hippocampal synapses [24]. Synapsin I-knockout mice show a severe epileptic phenotype without gross alterations in brain morphology and connectivity [25]. The dominant influence of synapsin I deletion on inhibitory transmission is thought to be attributed to the high-frequency firing characteristics of GABAergic interneurons. Thus, transcription of the synapsin I gene is likely to be more enhanced in inhibitory neurons than in excitatory neurons, which could account for preferential activation of the SynI-minCMV promoter in inhibitory rather than excitatory neurons.

5. Conclusions

In this study, we examined the transduction characteristics of systemically injected AAV-PHP.eB carrying neuron-specific CaMKII, NSE, or SynI-minCMV promoter. All three promoters displayed comparative or superior promoter strength over the ubiquitous CBh promoter. Among the three neuron-specific promoters tested, the NSE promoter exhibited the highest promoter activity. The 1.3-kb CaMKII promoter, which is generally considered to be excitatory neuron-specific, transduced both excitatory and inhibitory neurons without significant excitatory or inhibitory neuron bias, suggesting that the CaMKII promoter can be used as a neutral neuron-specific promoter. Conversely, the NSE promoter and SynI-minCMV promoter-transduced inhibitory neurons had a higher proportion of their natural presence, suggesting that these promoters serve as inhibitory neuron-preferential promoters. E/I imbalance in the cerebral cortex plays a key role in various neuropsychiatric disorders, including schizophrenia and autism [26–28]. Hence, the present results on the transduction characteristics of neuron-specific promoters may have particular implications when conducting neuropsychiatric behavioral experiments after systemic administration of BBB-penetrating AAV vectors carrying the neuron-specific promoter.

Funding

This work was supported by the Japan Society for the Promotion of Science (JSPS) KAKENHI Grants [Number 16K15477, and 18H02521] and grants from the program for Brain Mapping by Integrated Neurotechnologies for Disease Studies (Brain/MINDS) from the Japan Agency for Medical Research and Development (AMED) [Number JP20dm0207057/ JP21dm0207111] (to H. Hirai). This work was also supported by JSPS KAKENHI [Number 19K06899] (to A. Konno).

CRediT authorship contribution statement

Putri T. Radhiyanti: Formal analysis, Investigation, Writing - original draft. **Ayumu Konno:** Conceptualization, Writing - original draft. **Yasunori Matsuzaki:** Conceptualization. **Hirokazu Hirai:** Conceptualization, Writing - review & editing, Supervision.

Declaration of Competing Interest

The authors report no declarations of interest

Acknowledgements

The authors thank Asako Ohnishi, Nobue Mc Cullough, and Ayako Sugimoto for AAV vector production, and Junko Sugiyama for raising the mice. The authors would like to thank Editage (www.editage.com) for English language editing.

Appendix A. Supplementary data

Supplementary material related to this article can be found, in the online version, at doi:https://doi.org/10.1016/j.neulet.2021.135956.

References

[1] E. Zinn, L.H. Vandenberghe, Adeno-associated virus: fit to serve, Curr. Opin. Virol. 8 (2014) 90–97.
[2] S. Pillay, J.E. Carette, Host determinants of adeno-associated viral vector entry, Curr. Opin. Virol. 24 (2017) 124–131.
[3] D.F. Aschauer, S. Kreuz, S. Rumpel, Analysis of transduction efficiency, tropism and axonal transport of AAV serotypes 1, 2, 5, 6, 8 and 9 in the mouse brain, PLoS One 8 (2013), e76310.
[4] H. Monai, M. Ohkura, M. Tanaka, Y. Oe, A. Konno, H. Hirai, K. Mikoshiba, S. Itohara, J. Nakai, Y. Iwai, H. Hirase, Calcium imaging reveals glial involvement in transcranial direct current stimulation-induced plasticity in mouse brain, Nat. Commun. 7 (2016), 11100.
[5] Y. Shinohara, A. Konno, N. Takahashi, Y. Matsuzaki, S. Kishi, H. Hirai, Viral vector-based dissection of marmoset GFAP promoter in mouse and marmoset brains, PLoS One 11 (2016), e0162023.
[6] B.E. Deverman, P.L. Pravdo, B.P. Simpson, S.R. Kumar, K.Y. Chan, A. Banerjee, W. L. Wu, B. Yang, N. Huber, S.P. Pasca, V. Gradinaru, Cre-dependent selection yields AAV variants for widespread gene transfer to the adult brain, Nat. Biotechnol. 34 (2016) 204–209.
[7] K.Y. Chan, M.J. Jang, B.B. Yoo, A. Greenbaum, N. Ravi, W.L. Wu, L. Sánchez-Guardado, C. Lois, S.K. Mazmanian, B.E. Deverman, V. Gradinaru, Engineered AAVs for efficient noninvasive gene delivery to the central and peripheral nervous systems, Nat. Neurosci. 20 (2017) 1172–1179.
[8] M.H. Crommentuijn, R. Kantar, D.P. Noske, W.P. Vandertop, C.E. Badr, T. Würdinger, C.A. Maguire, B.A. Tannous, Systemically administered AAV9-sTRAIL combats invasive glioblastoma in a patient-derived orthotopic xenograft model, Mol. Ther. Oncolytics 3 (2016) 16017.
[9] R. Holehonnur, S.K. Lella, A. Ho, J.A. Luong, J.E. Ploski, The production of viral vectors designed to express large and difficult to express transgenes within neurons, Mol. Brain 8 (2015) 12.
[10] I. Scheyltjens, M.E. Laramée, C. Van den Haute, R. Gijsbers, Z. Debyser, V. Baekelandt, S. Vreysen, L. Arckens, Evaluation of the expression pattern of rAAV2/1, 2/5, 2/7, 2/8, and 2/9 serotypes with different promoters in the mouse visual cortex, J. Comp. Neurol. 523 (2015) 2019–2042.
[11] R. Kaneko, Y. Takatsuru, A. Morita, I. Amano, A. Haijima, I. Imayoshi, N. Tamamaki, N. Koibuchi, M. Watanabe, Y. Yanagawa, Inhibitory neuron-specific Cre-dependent red fluorescent labeling using VGAT BAC-based transgenic mouse lines with identified transgene integration sites, J. Comp. Neurol. 526 (2018) 373–396.
[12] Y. Shinohara, T. Ohtani, A. Konno, H. Hirai, Viral vector-based evaluation of regulatory regions in the neuron-specific enolase (NSE) promoter in mouse cerebellum in vivo, Cerebellum (London, England) 16 (2017) 913–922.
[13] A. Konno, H. Hirai, Efficient whole brain transduction by systemic infusion of minimally purified AAV-PHP.eB, J. Neurosci. Methods 346 (2020), 108914.
[14] R.D. Dayton, M.S. Grames, R.L. Klein, More expansive gene transfer to the rat CNS: AAV PHP.EB vector dose-response and comparison to AAV PHP.B, Gene Ther. 25 (2018) 392–400.
[15] T. Dittgen, A. Nimmerjahn, S. Komai, P. Licznerski, J. Waters, T.W. Margrie, F. Helmchen, W. Denk, M. Brecht, P. Osten, Lentivirus-based genetic manipulations of cortical neurons and their optical and electrophysiological monitoring in vivo, Proc. Natl. Acad. Sci. U. S. A. 101 (2004) 18206–18211.
[16] Y. Matsuzaki, M. Oue, H. Hirai, Generation of a neurodegenerative disease mouse model using lentiviral vectors carrying an enhanced synapsin I promoter, J. Neurosci. Methods 223 (2014) 133–143.
[17] J.J.J. Hjorth, A. Kozlov, I. Carannante, J. Frost Nylén, R. Lindroos, Y. Johansson, A. Tokarska, M.C. Dorst, S.M. Suryanarayana, G. Silberberg, J. Hellgren Kotaleski, S. Grillner, The microcircuits of striatum in silico, Proc. Natl. Acad. Sci. U. S. A. 117 (2020) 9554–9565.
[18] S.J. Gray, V. Matagne, L. Bachaboina, S. Yadav, S.R. Ojeda, R.J. Samulski, Preclinical differences of intravascular AAV9 delivery to neurons and glia: a comparative study of adult mice and nonhuman primates, Mol. Ther. 19 (2011) 1058–1069.
[19] J.L. Nathanson, Y. Yanagawa, K. Obata, E.M. Callaway, Preferential labeling of inhibitory and excitatory cortical neurons by endogenous tropism of adeno-associated virus and lentivirus vectors, Neuroscience 161 (2009) 441–450.
[20] A.I. Gulyás, G.G. Szabó, I. Ulbert, N. Holderith, H. Monyer, F. Erdélyi, G. Szabó, T. F. Freund, N. Hájos, Parvalbumin-containing fast-spiking basket cells generate the field potential oscillations induced by cholinergic receptor activation in the hippocampus, J. Neurosci. 30 (2010) 15134–15145.
[21] O. Kann, The interneuron energy hypothesis: implications for brain disease, Neurobiol. Dis. 90 (2016) 75–85.
[22] G. Ashrafi, T.A. Ryan, Glucose metabolism in nerve terminals, Curr. Opin. Neurobiol. 45 (2017) 156–161.
[23] J.O. Hollnagel, T. Cesetti, J. Schneider, A. Vazetdinova, F. Valiullina-Rakhmatullina, A. Lewen, A. Rozov, O. Kann, Lactate attenuates synaptic transmission and affects brain rhythms featuring high energy expenditure, iScience 23 (2020), 101316.
[24] S. Terada, T. Tsujimoto, Y. Takei, T. Takahashi, N. Hirokawa, Impairment of inhibitory synaptic transmission in mice lacking synapsin I, J. Cell Biol. 145 (1999) 1039–1048.
[25] A. Fassio, A. Raimondi, G. Lignani, F. Benfenati, P. Baldelli, Synapsins: from synapse to network hyperexcitability and epilepsy, Semin. Cell Dev. Biol. 22 (2011) 408–415.
[26] Y. Bozzi, G. Provenzano, S. Casarosa, Neurobiological bases of autism-epilepsy comorbidity: a focus on excitation/inhibition imbalance, Eur. J. Neurosci. 47 (2018) 534–548.
[27] B.R. Ferguson, W.J. Gao, PV interneurons: critical regulators of E/I balance for prefrontal cortex-dependent behavior and psychiatric disorders, Front. Neural Circuits 12 (2018) 37.
[28] V.S. Sohal, J.L.R. Rubenstein, Excitation-inhibition balance as a framework for investigating mechanisms in neuropsychiatric disorders, Mol. Psychiatry 24 (2019) 1248–1257.